LA-UR-04-7215

Approved for public release;
distribution is unlimited.

Title: Transient Loads Identification for a Standoff Metallic Thermal Protection System Pane

Author(s):
R . Jason Hundhausen,
Douglas E . Adams, Purdue University
Mark Derriso , Air Force Research Laboratory, Wright-Patterson AFB
Paul Kukuchek, Goodrich Aerostructures
Richard Alloway , Goodrich Aerostructures

Intended for:
Society for Experimental Mechanics (SEM)
International Modal Analysis Conference
1 /31 /05 - 2/3/05
Orlando, FL

Transient Loads Identification for a Standoff Metallic Thermal Protection System Panel

R. Jason Hundhausen[1], Douglas E. Adams[2], Mark Derriso[3], Paul Kukuchek[4], Richard Alloway[4]

[1]Engineering Sciences and Applications, Weapon Response Group, MS T001, Los Alamos National Laboratory, Los Alamos, NM 87545

[2]School of Mechanical Engineering, Ray W. Herrick Laboratories, Purdue University, 140 S. Intramural Drive, West Lafayette, IN, 47907-2031

[3]Air Vehicles Directorate, Structures Division, Air Force Research Laboratory, 2790 D. Street, WPAFB, OH, 45433

[4]Research and Development, MZ 107P, Goodrich Aerostructures, 850 Lagoon Dr, Chula Vista, CA 91910

ABSTRACT

Standoff thermal protection system (TPS) panels are critical structural components in future aerospace vehicles because they protect the vehicle from the hostile environment encountered during space launch and reentry. Consequently, the panels are exposed to a variety of loads including high temperature thermal stresses, thermal shock, acoustic pressure, and foreign object impacts. Transient impacts are especially detrimental because they can cause immediate and severe degradation of the panel in the form of, for example, debonding and buckling of the face sheet, cracking of the fasteners, or deformation of the standoffs. Loads identification methods for determining the magnitude and location of impact loads provide an indication of TPS components that may be more susceptible to failure. Furthermore, a historical database of impact loads encountered can be retained for use in the development of statistical models that relate impact loading to panel life. In this work, simulated in-service transient loads are identified experimentally using two methods: a physics-based approach and an inverse Frequency Response Function (FRF) approach. It is shown that by applying the inverse FRF method, the location and magnitude of these simulated impacts can be identified with a high degree of accuracy. The identified force levels vary significantly with impact location due to the differences in panel deformation at the impact site indicating that resultant damage due to impacts would vary with location as well.

1. INTRODUCTION

Foreign object impact identification is an essential part of a thermal protection system (TPS) structural health monitoring (SHM) system because impacts can instantaneously produce damage in TPS materials and structures. Loads identification is the process of determining the magnitude and location of (impact) loads acting on the TPS panels and is the first step in TPS SHM because this information can be used to identify areas of the TPS that may be more susceptible to damage. Once these "hot-spots" are identified, immediate assessments of TPS health can be made and future off-line NDT inspections can be scheduled. Two approaches for loads identification are described in this work: a kinematics-based approach and an inverse Frequency Response Function (FRF) approach.

1.1. Previous Work

Many scientists and engineers have worked to identify external structural loads. There are several technical issues that arise when estimating external loads given a limited set of response measurements. First, this problem is an ill-conditioned inverse problem with no unique solution because the system response is generally a continuous function of the spatial coordinates, whereas the measured response is defined only at a few discrete points [1]. Second, solutions are often highly sensitive to small amounts of signal noise. Third, spatial aliasing can occur if there are poorly placed or too few sensors leading to incorrect approximated response fields.

There are many techniques that have been developed for loads identification. In 1990, Dobson and Rider [2] published a review detailing the frequency domain model, modal model, and finite element model techniques. Works on indirect force measurement, where the location of the force is known a priori can be found in, for

example, Carne et al. [3,4], Fabunmi [5], Hansen and Starkey [6], Hillary and Ewins [7], Hollandsworth and Busby [8], Law et al. [9], Lee and Park [10], Verhoeven [11], Yu and Chan [12], Zhu and Law [13,14], and Zhu and Lu [15]. Works that pertain to identification of loads where the location of the applied load is also unknown can be found in, for example, Möller [1], D'Cruz et al. [16], Yanyutin and Voropai [17], Sydel and Chang [18-20], Tracy and Chang [21], Choi and Chang [22]. Shih et al. [23] and Zhang et al. [24] also studied the possibility of determining the number of potentially incoherent loads acting on a structure. Studies that pertain to ill-conditioning and various techniques to alleviate such problems (e.g. regularization, see Zhu and Law [13,14], Lee and Park [10], and Tikhonov and Arsenin [25]) can be found in Hillary and Ewins [7], Okubo et al. [26], Hansen and Starkey [6], and Karlsson [27].

Of particular pertinence to this work are several papers that pertain to the use of frequency domain methods (see, e.g. [5,28-32]), which have shown that this approach can be highly sensitive to small perturbations in response measurements and can easily result in ill-conditioning of the Frequency Response Function matrix. One approach to reducing this problem is to over-define the problem, i.e. measure the response at more points than there are input points [29]; however, this approach can be impractical for situations where there are many input locations and few places to measure the response. Giasante et al. [32] studied the rotor hub loads of a helicopter during flight. They measured the response with 37 accelerometers, given four single-frequency excitation forces whose location was known a priori. The forces that were computed from the in-flight tests were then applied to the helicopter during ground tests. A high degree of correlation was noted between the in-flight and ground test response. Similarly, Kinns et al. [33] used the same method to estimate the magnitude of the forces acting within a marine turbo-alternator. In their work, 12 accelerometers were used to estimate the variation in nine unknown forces acting on the alternator over an 18-month period. It was shown that the forces varied considerably; however, the precise cause for the changes in the estimated force magnitude were unknown. They postulated that the differences were a result of altered damping mechanisms present in the bearing oil films between on-ground stationary tests and in-flight running tests.

There has also been a good amount of work in impact loads identification in plates. Yanyutin and Voropai [17] present a method for deriving the equations of motion for a rectangular plate using Timoshenko plate theory, which accounts for transverse shear and rotary inertia effects, and apply an impulsive load to a small area of the plate (relative to the plate size). Given the differential equations of motion of the plate, they transform into an integral equation related to the impulsive loads, from which they solve a linear integral Volterra equation of the first kind. In order to solve the integral equation, they apply Tikhonov's regularization [34,35], which can account for errors on the measured response. They compared theoretical results to results from experiments where a ball was dropped on the plate. Minor differences aside, the results between theoretical and experimental showed positive correlation. It is important to note that the location of the applied load was known beforehand. Tracy and Chang [21] present an algorithm for determining both the magnitude and location of impulsive loads applied to a 36-inch by 30-inch composite plate. In this work, they use a set of 13 distributed piezoelectric elements as sensors and compare the estimated dynamic response of the plate to that which was measured. A computer was used to iteratively compare the actual and estimated responses, after which the model is updated until the actual response and estimated response match one another within a specified tolerance. They showed that their computer code could accurately identify both the magnitude and location of impulsive forces applied to the composite plate. One drawback to this system is the use of a rather high density of sensors. For more information on the method presented in [21], see references [18-20,22].

2. IDENTIFICATION OF EXTERNAL IMPULSIVE LOADS

2.1. Rigid Body Kinematics-Based Approach

The fundamental assumption behind the kinematics-based approach to loads identification presented here is the assumption that the panel behaves like a rigid body at low frequencies. With this assumption, Chasles' theorem can be applied. This theorem states that "The most general displacement of a rigid body is equivalent to a screw displacement," [36]. Paraphrasing, Chasles' theorem indicates that every rigid body motion can be realized by the sum of all rigid body translations and rotations about an axis. Eq. (1) describes this relationship between a perimeter point motion and the motion of the center of mass:

$$\begin{Bmatrix} \ddot{x}_p \\ \ddot{y}_p \\ \ddot{z}_p \end{Bmatrix}_{3\times1} = \begin{bmatrix} 1 & 0 & 0 & 0 & z_{p,cm} & -y_{p,cm} \\ 0 & 1 & 0 & -z_{p,cm} & 0 & x_{p,cm} \\ 0 & 0 & 1 & y_{p,cm} & -x_{p,cm} & 0 \end{bmatrix}_{3\times6} \begin{Bmatrix} \ddot{X} \\ \ddot{Y} \\ \ddot{Z} \\ \ddot{\Theta}_x \\ \ddot{\Theta}_y \\ \ddot{\Theta}_z \end{Bmatrix}^{CM}_{6\times1}, \tag{1}$$

$$\{\ddot{x}_p\}_{3\times1} = [T_R]_{3\times6} \{\ddot{R}\}_{6\times1}$$

where p is a point on the body, $\{\ddot{R}\}$ is a vector describing the motion of the center of mass (CM), the double dot signifies the second spatial derivative with respect to time and $x_{p,cm}$, $y_{p,cm}$ and $z_{p,cm}$ are the coordinates of point p relative to the CM (Figure 1).

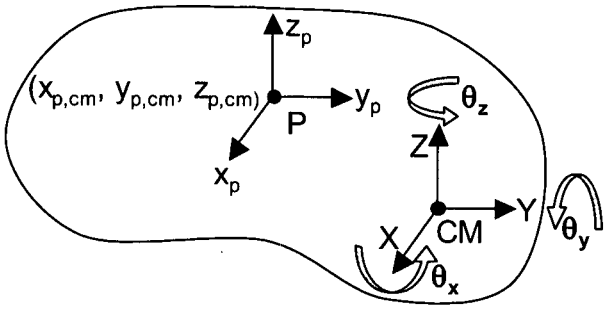

Figure 1: Relationship of Perimeter Point Motion to Center of Mass Motion.

Thus, if the motion of the CM is known, the motion of any perimeter point can be calculated [37]. However, the reverse problem – calculating the motion of the CM given the motion at a single point p – results in an underdetermined system: 6 unknowns in 3 equations. This problem of having too few equations can be alleviated by measuring the response at multiple points on the panel and using a least-squares approximation to invert $[T_R]$:

$$\begin{bmatrix} [T_R^1] \\ [T_R^2] \\ \vdots \\ [T_R^n] \end{bmatrix}^{\dagger}_{6\times3n} \begin{Bmatrix} \{\ddot{x}_1\} \\ \{\ddot{x}_2\} \\ \vdots \\ \{\ddot{x}_n\} \end{Bmatrix}_{3n\times1} \cong \begin{Bmatrix} \ddot{X} \\ \ddot{Y} \\ \ddot{Z} \\ \ddot{\Theta}_x \\ \ddot{\Theta}_y \\ \ddot{\Theta}_z \end{Bmatrix}^{CM}_{6\times1}, \tag{2}$$

where n denotes the number of response points, and $[T_R]^{\dagger}$ denotes the pseudoinverse of $[T_R]$. The pseudoinverse function is based on the minimization of the least-squared error in a set of linear equations and is sometimes referred to as the minimal norm least squares solution.

Once the motion of the CM is known, the Newton-Euler equations can be implemented to determine an equivalent force-moment couple acting at the CM using the following equation of motion:

$$\begin{Bmatrix} F_x \\ F_y \\ F_z \\ M_x \\ M_y \\ M_z \end{Bmatrix}^{CM}_{6\times1} = \begin{bmatrix} m & 0 & 0 & 0 & 0 & 0 \\ 0 & m & 0 & 0 & 0 & 0 \\ 0 & 0 & m & 0 & 0 & 0 \\ 0 & 0 & 0 & I_{xx} & I_{xy} & I_{xz} \\ 0 & 0 & 0 & I_{yx} & I_{yy} & I_{yz} \\ 0 & 0 & 0 & I_{zx} & I_{zy} & I_{zz} \end{bmatrix}_{6\times6} \begin{Bmatrix} \ddot{X} \\ \ddot{Y} \\ \ddot{Z} \\ \ddot{\Theta}_x \\ \ddot{\Theta}_y \\ \ddot{\Theta}_z \end{Bmatrix}^{CM}_{6\times1}, \tag{3}$$

where F_x, F_y, F_z, M_x, M_y, and M_z, are the equivalent forces and moments acting at the CM (respectively), m is the mass of the panel, and the I_{ij} ; $i,j=\{x,y,z\}$ terms are the mass-moments of inertia.

In the case of the TPS panel, the only moments acting on the system are in the form of couples (due to the standoff forces and impact forces), so in order to determine those loads, the equivalent force-moment couple acting at the CM must be replaced by a general forcing distribution that encompasses the force contributions from the standoffs and the foreign object impact. The relationship between the force-moment couple acting at the CM and the perimeter forces is given by

$$\begin{Bmatrix} F_x \\ F_y \\ F_z \\ M_x \\ M_y \\ M_z \end{Bmatrix}^{CM}_{6\times1} = \begin{bmatrix} 1 & 0 & 0 \\ 0 & 1 & 0 \\ 0 & 0 & 1 \\ 0 & -z_{p,cm} & y_{p,cm} \\ z_{p,cm} & 0 & -x_{p,cm} \\ -y_{p,cm} & x_{p,cm} & 0 \end{bmatrix}_{6\times3} \begin{Bmatrix} f_x \\ f_y \\ f_z \end{Bmatrix}^{p}_{3\times1}, \tag{4}$$

$$\{F_R\}^{CM}_{6\times1} = \left[T_F^p\right]_{6\times3} \{F^p\}_{3\times1}$$

where f_x, f_y and f_z are the forces acting at point p on the panel. An issue arises when attempting to solve the reverse of Eq. (4); in the case of the TPS panel, there are forces acting at five points on the panel: three orthogonal forces at each corner due to the standoffs and three forces acting at some unknown point due to the impact. In all, there are 17 unknowns: 15 unknown forces and two impact locations (the z coordinate of the impact is zero) in only six equations. A solution to this problem of too few equations is to directly calculate the stiffness of each standoff. By multiplying the stiffness at the standoffs by the standoff displacements (obtained by twice integrating the acceleration response at each standoff), 12 of the unknowns are eliminated leaving the three unknown impact forces and two impact locations to be determined.

2.2. Inverse Frequency Response Function Approach

An alternative approach to the kinematics-based approach to loads identification is the inverse FRF method. The FRF is analogous to the impedance of an electrical circuit; it is a relationship between the effort (e.g. voltage) and the flow (e.g. current) through the circuit as a function of frequency. In structural dynamics, the FRF is defined as the ratio between the response and the input of the system as a function of frequency. This relationship is given by

$$\{X\}_{p\times 1} = [H]_{p\times q}\{F\}_{q\times 1}, \tag{5}$$

where *{X}* is the response of the system at response DOFs *p*; *{F}* is the input to the system at input DOFs *q*; and *[H]* is the system impedance, or FRF. The inverse FRF approach uses the FRF as a "fingerprint" of the system, i.e., measure the FRF of a system and use the FRF, in conjunction with measured response, to identify loads acting on the system. This approach can be expressed in equation form as

$$\left\{\hat{F}\right\}_{q\times 1} = \left[H^{\dagger}\right]_{q\times p}\{X\}_{p\times 1} = \left(\left[H^{*T}\right]_{q\times p}[H]_{p\times q}\right)^{-1}_{q\times q}\left[H^{*T}\right]_{q\times p}\{X\}_{p\times 1}, \tag{6}$$

where $[H]^{\dagger}$ denotes the pseudoinverse of *[H]* and $[H^{*T}]$ is the complex conjugate transpose of *[H]*. The use of a pseudoinverse is necessary if *[H]* is not square, but the number of response DOFs (*p*) must be greater than or equal to the number of input DOFs (*q*) to avoid erroneous results. Theoretically, the number of response DOFs need only equal the number of input DOFs; however, because experimental measurements are often subject to slight errors and inconsistencies, many more response DOFs than input DOFs should be used to solve for the forces acting on the system with a least-squares algorithm such as the pseudoinverse [29,32]. One drawback to this approach is that at each arbitrary frequency, the *qxq* size matrix must be inverted, resulting in decreased computational efficiency when *q* or the number of discrete frequencies becomes large.

3. EXPERIMENTAL VERIFICATION OF TECHNIQUES

Experimental impact tests were performed to confirm the validity of the kinematics-based and inverse FRF approaches. Two sets of tests were performed; the first was designed around the kinematics-based approach to loads identification and involved impacting the panel at nine different locations and measuring the time-domain response at the standoff locations. The second test was designed around the inverse FRF approach to loads identification and involved an identical testing regimen as the kinematics-based approach, but instead of collecting time histories, the FRFs were measured.

3.1. Kinematics-Based Approach Experimental Results

Impacts were made with a TMS 086M92 electric impact hammer at nine points on the panel. The response (x, y and z direction) was measured at each standoff location (points one, two, three, and four) on the panel with PCB T356B18 tri-axial accelerometers (Figure 2).

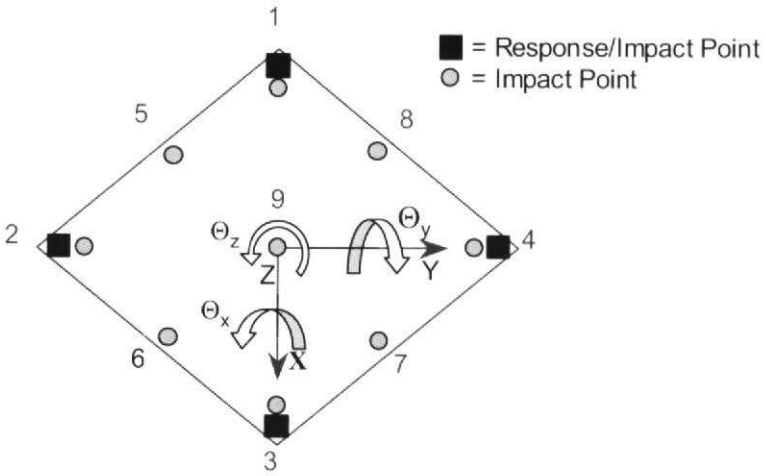

Figure 2: Panel Impact and Response Points.

The TPS panel was mounted to a 500-pound steel test table that was designed to provide a rigid stationary boundary condition. Figure 3 shows the experimental testing fixture and accelerometers used. The electric impact hammer was fitted with a PCB 288C01 force/acceleration impedance head with a delrin tip to provide a 10 dB roll-off in the input power spectrum out to 400 Hz.

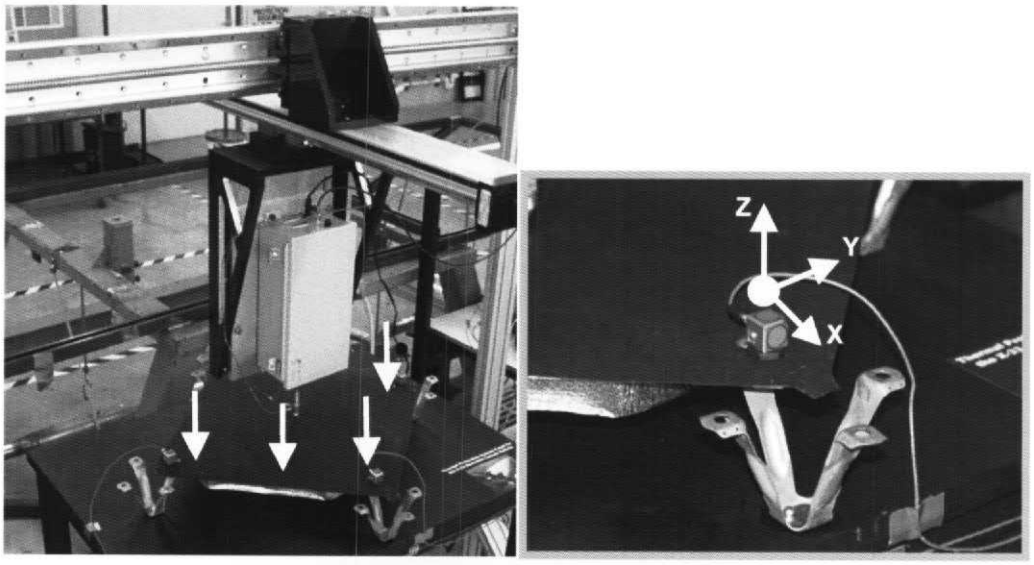

Figure 3: Experimental Impact Testing Fixture and Accelerometer.

Data were collected with a 16 channel IOTech WavePort™ data acquisition system. Eight seconds of data were recorded at a sample rate of 8,192 Hz. Subsequent signal processing was performed with MATLAB®.

By measuring the response at four points on the panel, the motion of the CM could be found by rewriting Eq. (2) as:

$$\left[\begin{bmatrix} 1 & 0 & 0 & 0 & \cancel{z_{1,cm}} & -y_{1,cm} \\ 0 & 1 & 0 & \cancel{-z_{1,cm}} & 0 & x_{1,cm} \\ 0 & 0 & 1 & y_{1,cm} & -x_{1,cm} & 0 \end{bmatrix} \begin{bmatrix} 1 & 0 & 0 & 0 & \cancel{z_{2,cm}} & -y_{2,cm} \\ 0 & 1 & 0 & -z_{2,cm} & 0 & x_{2,cm} \\ 0 & 0 & 1 & \cancel{y_{2,cm}} & -x_{2,cm} & 0 \end{bmatrix} \begin{bmatrix} 1 & 0 & 0 & 0 & \cancel{z_{3,cm}} & -y_{3,cm} \\ 0 & 1 & 0 & \cancel{-z_{3,cm}} & 0 & x_{3,cm} \\ 0 & 0 & 1 & y_{3,cm} & -x_{3,cm} & 0 \end{bmatrix} \begin{bmatrix} 1 & 0 & 0 & 0 & \cancel{z_{4,cm}} & -y_{4,cm} \\ 0 & 1 & 0 & \cancel{-z_{4,cm}} & 0 & x_{4,cm} \\ 0 & 0 & 1 & y_{4,cm} & -x_{4,cm} & 0 \end{bmatrix}\right]^{\dagger}_{6\times 12} \begin{Bmatrix} \begin{Bmatrix} \ddot{x}_1 \\ \ddot{y}_1 \\ \ddot{z}_1 \end{Bmatrix} \begin{Bmatrix} \ddot{x}_2 \\ \ddot{y}_2 \\ \ddot{z}_2 \end{Bmatrix} \begin{Bmatrix} \ddot{x}_3 \\ \ddot{y}_3 \\ \ddot{z}_3 \end{Bmatrix} \begin{Bmatrix} \ddot{x}_4 \\ \ddot{y}_4 \\ \ddot{z}_4 \end{Bmatrix} \end{Bmatrix}_{12\times 1} \cong \begin{Bmatrix} \ddot{X} \\ \ddot{Y} \\ \ddot{Z} \\ \ddot{\Theta}_x \\ \ddot{\Theta}_y \\ \ddot{\Theta}_z \end{Bmatrix}^{CM}_{6\times 1}, \tag{7}$$

where the subscripts, *1*, *2*, *3* and *4* denote location on the panel and $x_{1,cm}$, $y_{1,cm}$, $z_{1,cm}$,..., $x_{4,cm}$, $y_{4,cm}$, $z_{4,cm}$ are the locations of the response points in relation to the CM ($z_{1,cm}$,..., $z_{4,cm}$ are zero in the case of this flat panel). A trial was formulated to verify that the results of applying a pseudoinverse produced a reasonable approximation of the motion of the CM (Figure 4). Beginning with the perimeter response measurements, Eq. (2) was applied to generate an estimation of the CM motion; then the estimated CM motion was used along with Eq. (1) to calculate the perimeter motions; finally, these estimated perimeter motions were compared with the original response measurements. If the pseudoinverse is generating the correct CM motion, the two results should be identical (minor differences notwithstanding). Figure 5 shows one example of a comparison of the measured and estimated response; in all cases the correlation between the two plots was reasonably good. The error in the beginning of the time history shown in Figure 5 is due to contributions from non rigid-body (flexible) motions of the panel immediately following the impact. It is believed that the panel motions were consistently underestimated in magnitude as in Figure 5 due to a bias error in the location of the CM and perhaps some residual flexible body motions in the time history.

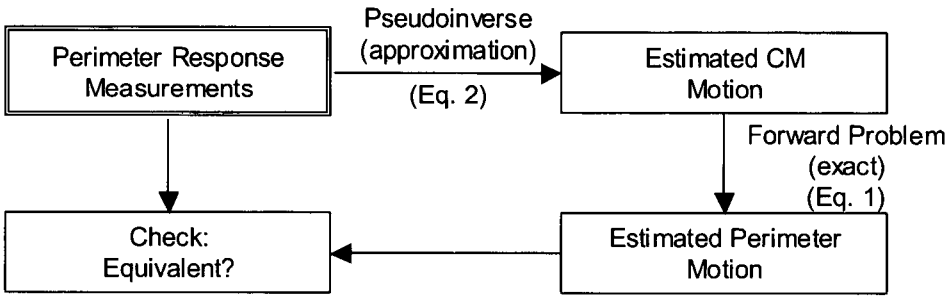

Figure 4: Pseudoinverse Trial Flowchart.

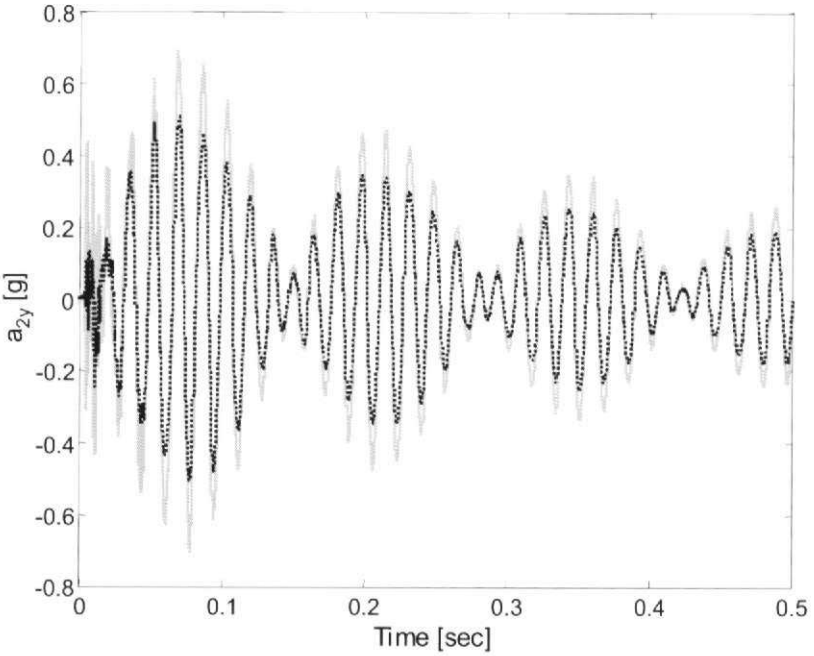

Figure 5: Comparison of Measured Perimeter Response (—) and Estimated Perimeter Response (····) Using Pseudoinverse.

A dimensioned, three-dimensional solid model of the panel was created with Pro/E® CAD software to determine the total mass and inertia tensors of the panel. These inertial properties were needed in order to calculate the equivalent force-moment couple acting at the CM. A technique was applied in which the location of the impact was assumed to be one of the nine points on the panel shown in Figure 2. This technique effectively partitioned the panel into nine regions (local to each point) where the impact forces were then calculated. A plot of the maximum estimated impact force versus panel location is shown in Figure 6. Each series in Figure 7 represents the maximum estimated impact when that impact is assumed to be acting at one point (in the vertical direction) on the panel. For example, if the response of the system is measured when an impact occurs at point three, and the impact force is assumed to act (successively) at points one through nine, the maximum estimated impact force in the series should correspond to location three on the panel. The other "hump" in Figure 6 near points six and seven is thought to emerge in the estimated force because of the proximity of these points to the impact point (three); however, the relatively high estimated force near points eight and nine cannot be explained in this way.

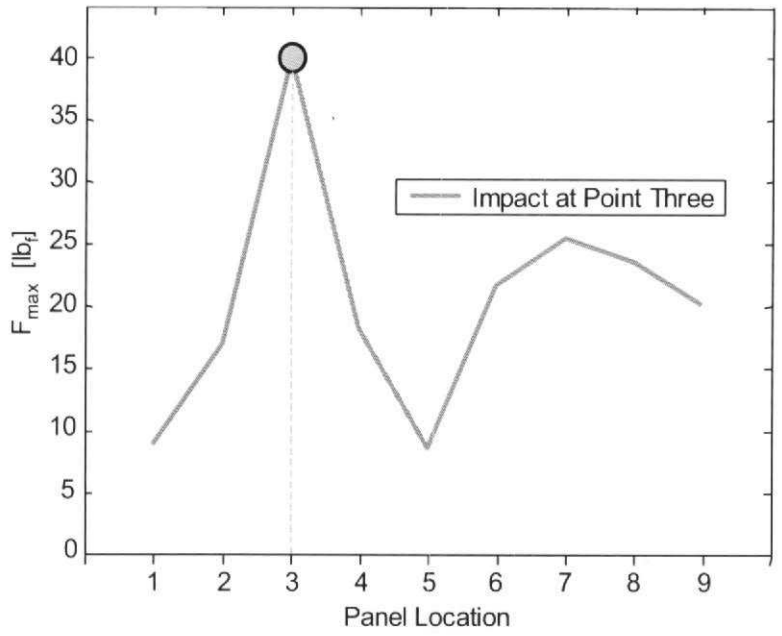

Figure 6: Maximum Estimated Impact Force versus Panel Location for an Impact at Point Three.

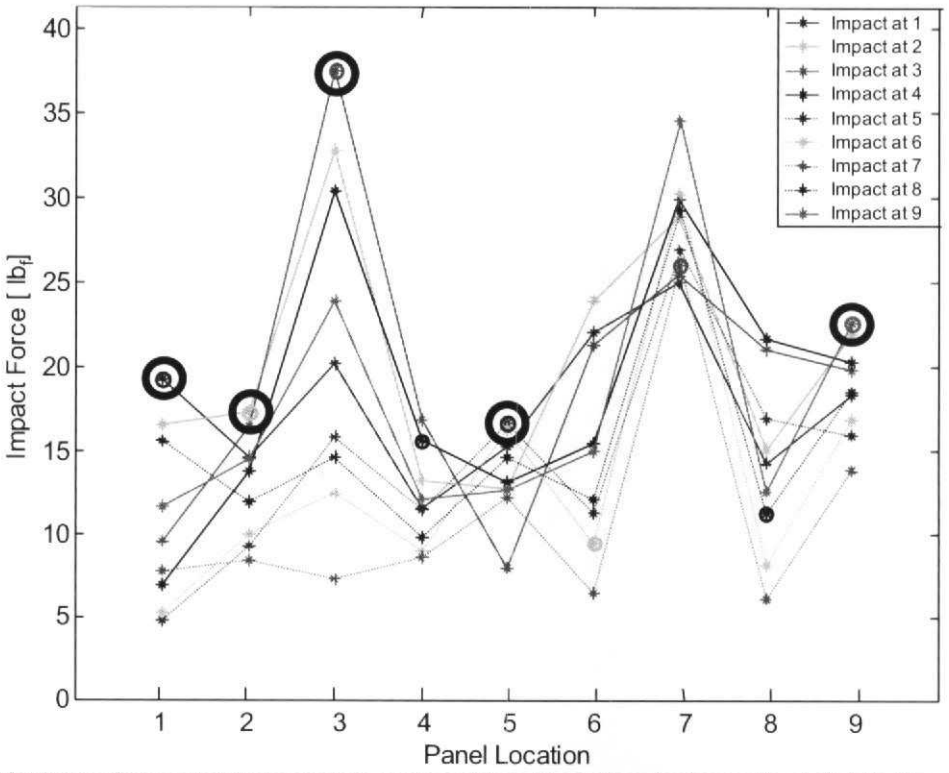

Figure 7: Maximum Estimated Impact Force versus Panel Location for Impacts at Points One Through Nine.

In five out of the nine cases the location of the impact was properly identified (Figure 7 (○)); none of the cases properly identified the impact magnitude. In eight out of nine cases the impact force was underestimated. There are several reasons for these errors. The first reason is that the assumption of rigid-body behavior is invalid and

that the effects of panel flexural modes are distorting the results. The second reason is that the standoffs were assumed to behave as springs with no dampers; this assumption would tend to result in an under-prediction of the impact forces. The third reason is that the amplitude of response was consistently underestimated as was shown in Figure 5; therefore, the force would consequently be underestimated. The final reason is that all of the impact tests were performed without ensuring than an even preload was present in all bolts, and, given the inherent nonlinear behavior of bolted joints, any perturbations in bolt preload would distort the effective stiffness of the standoffs.

3.2. Inverse Frequency Response Approach Experimental Results

To determine the FRF matrix, impacts were performed on the TPS panel at the nine points shown in section 3.1, Figure 2; in this set of experiments, the preload of the fasteners was set to 90 (± 0.25) inch-lb_f of torque. Data were collected with a 16 channel Agilent 1401/1432 51.6 kHz VXI data acquisition system. The MRIT-VXI data acquisition software was used to obtain the FRFs between each accelerometer response and the corresponding input for each impact location. Fifteen linear spectral averages were taken at each impact location using a force-exponential window on each set of measured data.

When the FRFs for each input/output pair were assembled into matrix form and placed into Eq. (5), the following expression was obtained:

$$\begin{Bmatrix} X_{1x} \\ X_{1y} \\ X_{1z} \\ X_{2x} \\ \vdots \\ X_{4z} \end{Bmatrix}_{12\times 1} = \begin{bmatrix} H_{1x,1z} & H_{1x,2z} & H_{1x,3z} & H_{1x,4z} & \cdots & H_{1x,9z} \\ H_{1y,1z} & H_{1y,2z} & H_{1y,3z} & H_{1y,4z} & \cdots & H_{1y,9z} \\ H_{1z,1z} & H_{1z,2z} & H_{1z,3z} & H_{1z,4z} & \cdots & H_{1z,9z} \\ H_{2x,1z} & H_{2x,2z} & H_{2x,3z} & H_{2x,4z} & \cdots & H_{2x,9z} \\ \vdots & \vdots & \vdots & \vdots & \ddots & \vdots \\ H_{4z,1z} & H_{4z,2z} & H_{4z,3z} & H_{4z,4z} & \cdots & H_{4z,9z} \end{bmatrix}_{12\times 9} \begin{Bmatrix} F_{1z} \\ F_{2z} \\ F_{3z} \\ F_{4z} \\ \vdots \\ F_{9z} \end{Bmatrix}_{9\times 1}, \tag{8}$$

where the X_{1x}, X_{1y}, X_{1z}, X_{2x},..., X_{4z} denote the acceleration response (in the frequency domain) at DOFs one through four and F_{1z}, F_{2z}, F_{3z},..., F_{9z} denote the input (in the frequency domain) at DOFs one through nine.

The time-domain response data collected in the impact tests described in section 3.1 could now be used in conjunction with the FRF matrix to identify the loads acting on the system. A brief summary of the MATLAB® code used in this process is described below:

1) Form the FRF matrix that was identified by the steps described above in section 3.2 above and insert the time-domain response data collected in the impact tests described in section 3.1.

2) Reconstruct the FRF matrix, *[H]*, to include both positive and negative frequency content. This reconstruction step is necessary because the MRIT data acquisition software only supplies the positive frequency information.

3) Perform a Discrete Fourier Transform (DFT) using the MATLAB® command *fft* to transform the time-domain impact test data into the frequency domain.

4) Multiply the frequency-domain response vector *{X}* by the pseudoinverse of *[H]* to obtain an approximation of the frequency-domain input force vector *{F}*.

5) Perform an Inverse Discrete Fourier Transform of *{F}* to transform *{F}* into the time domain.

The results of the inverse FRF method described above were found to be very good. Table 3.1 summarizes the results of the actual impact force comparison with the estimated impact force. The maximum error in impact force is 4.02 percent, a dramatic increase in accuracy over the kinematics-based approach.

Table 3.1: Actual and Estimated Impact Forces for Inverse Frequency Response Function Loads Identification.

Location	Measured Impact Force (lb_f)	Estimated Impact Force (lb_f)	Error (%)
1	23.369	23.201	-0.72
2	10.205	10.615	4.02
3	14.119	14.086	-0.23
4	14.819	14.805	-0.09
5	23.457	23.540	0.35
6	10.044	10.002	-0.42
7	9.763	9.784	0.22
8	8.292	8.461	2.04
9	15.168	14.863	-2.01

The location of the impact was correctly identified for all nine test locations (Figure 8). Additionally, the magnitude of each impact was calculated to a high degree of accuracy. Figure 9 shows a typical result of the comparison of the actual time-domain impact force with the estimated impact force; Figure 10 shows a side-by-side comparison of actual and estimated impact force. Note that for approximately the same impact energy at locations one through nine in Figure 10, there are significant differences in resultant maximum forces. A higher force would likely result in more potential for damage to the TPS. Therefore, it can be concluded that the variation in displacement at the nine different locations results in a different force and susceptibility to impact damage at the nine locations.

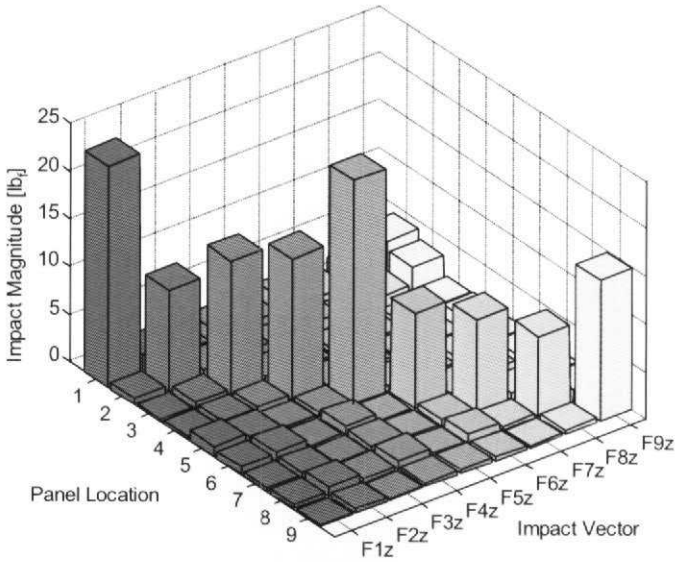

Figure 8: Correlation of Impact Vector Index with Panel Location and Impact Magnitude.

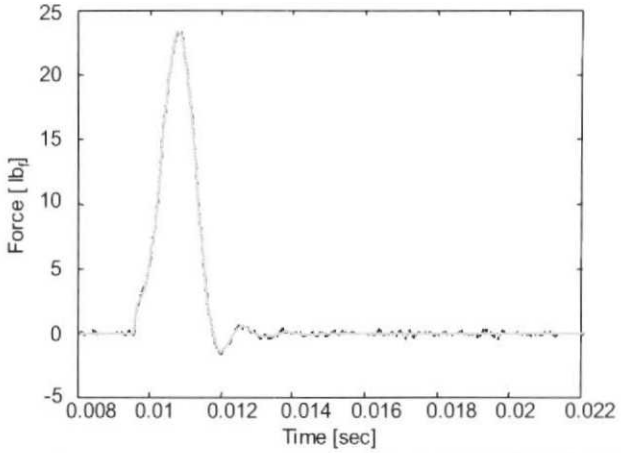

Figure 9: Typical Example of Actual Impact Time History (—) and Estimated Impact Time History (···).

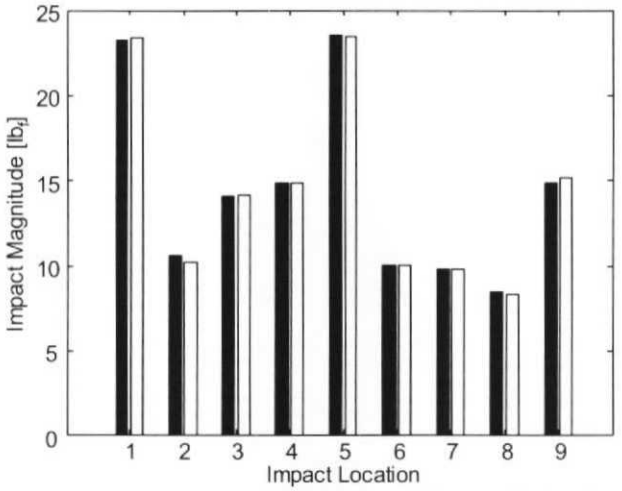

Figure 10: Comparison of Actual (□) and Estimated (▬) Impact Forces Using Inverse Frequency Response Function Approach.

4. CONCLUSIONS

One issue that future work in the area of loads identification will need to address is that the FRF only characterizes the original system for which the FRFs are computed. If the system is altered in any way, e.g., is *damaged*, the panel material properties change due to a significant increase in temperature, or the mass changes as a result of oxidation or nitridation, then the original FRF is no longer a valid identifier for the system. The second issue is that the FRF is a linear transfer function relating the input to a system to the response. For situations in which the loading is extreme, e.g., high velocity impacts and the 180 dB sound pressure levels experienced by these panels, the system will exhibit nonlinear behavior and again the FRF will no longer be valid. A third issue that these techniques must address in future work is that the impacts applied in the experiments described above were unidirectional and were only applied at points one through nine, not any points in-between. In future work, the effects of slight off-axis excitations (e.g., impact occurs at point three with components in the z direction and the x and y directions) and the effects of excitations applied at random locations on the panel on the accuracy of these results must be assessed. These issues aside, the results of the inverse FRF approach to loads identification are promising. It has been shown that impacts on a TPS panel can be located and quantified to a high degree of accuracy. Loads identification will provide invaluable information to the flight crew and ground inspectors because it will designate specific areas of the TPS that have been subjected to potentially detrimental loads.

5. ACKNOWLEDGEMENTS

The authors would like to express their gratitude to the Air Force Research Laboratory Air Vehicles Directorate at Wright-Patterson Air Force Base, Anteon Corporation, Goodrich Aerostructures Group for their generous donation of the metallic TPS panels, and PCB/The Modal Shop for their contribution of the electric impact hammer and force/acceleration impedance transducer used in these experiments.

6. REFERENCES

1. Möller, P.W., "Load Identification Through Structural Modification," March 1999, *Journal of Applied Mechanics, Transactions of ASME*, **66**(1), pp. 236-241.

2. Dobson, B. J. and Rider, E., "A Review of the Indirect Calculation of Excitation Forces from Measured Structural Response Data," 1990, *Proceedings of the Institution of Mechanical Engineers Part C: Journal of Mechanical Engineering Science, **204**(2), pp. 69-75.*

3. Carne, T. G., Bateman, V. I., and Mayes, R. L., "Force Reconstruction Using the Sum of Weighted Accelerations Technique," 1992, *Proceedings of the International Modal Analysis Conference*, pp. 291-298.

4. Carne, T. G., Mayes, R. L., and Bateman, V. I., "Force Reconstruction Using the Sum of Weighted Accelerations Technique – Max-Flat Procedure," 1994, *Proceedings of the International Modal Analysis Conference*, pp. 1054-1062.

5. Fabunmi, J. A., "Effects of Structural Modes on Vibratory Force Determination by the Pseudoinverse Technique," 1986, *American Institute of Aeronautics and Astronautics Journal*, **24**(3), pp. 504-509.

6. Hansen, M. and Starkey, J. M., "On Predicting and Improving the Condition of Modal-Model-Based Indirect Force Measurement Algorithms," 1990, *Proceedings of the International Modal Analysis Conference*, pp. 115-120.

7. Hillary, B. and Ewins, D. J., "The Use of Strain Gauges in Force Determination and Frequency Response Function Measurements," 1984, *Proceedings of the International Modal Analysis Conference*, **2**, pp. 627-634.

8. Hollandsworth, P. E. and Busby, H. R., "Impact Force Identification Using the General Inverse Technique," 1989, *International Journal of Impact Engineering*, **8**(4), pp. 315-322.

9. Law, S. S. and Chan, T. H. T., "Moving Force Identification: A Time Domain Method," 1997, *Journal of Sound and Vibration*, **201**(1), pp. 1-22.

10. Lee, H. and Park, Y-S., "Error Analysis of Indirect Force Determination and a Regularisation Method to Reduce Force Determination Error," 1995, *Mechanical Systems and Signal Processing*, **9**(6), pp. 615-633.

11. Verhoeven, J., "Excitation Force Identification of Rotating Machines Using Operational Rotor/Stator Amplitude Data and Analytical Synthesized Transfer Functions," July 1998, *Journal of Vibration, Acoustics, Stress, and Reliability in Design*, **110**(3), pp. 307-314.

12. Yu, L. and Chan, T. H. T., "Moving Force Identification Based on the Frequency-Time Domain Method," March 2003, *Journal of Sound and Vibration*, **261**(2), pp. 329-349.

13. Zhu, Z. Q. and Law, S. S., "Identification of Moving Loads on a Rectangular Orthotropic Plate from Strains," 2001, *Proceedings of the International Modal Analysis Conference*, **1**, pp. 158-164.

14. Zhu, Z. Q. and Law, S. S., "Moving Loads Identification Through Regularization," Sept. 2002, *Journal of Engineering Mechanics*, **128**(9), pp. 989-1000.

15. Zhu, J. and Lu, Z., "A Time Domain Method for Identifying Dynamic Loads on Continuous Systems," July 1991, *Journal of Sound and Vibration*, **148**(1), pp. 137-146.

16. D'Cruz, J., Crisp, J. D. C., and Ryall, T. G., "On the Identification of a Harmonic Force on a Viscoelastic Plate From Response Data," Dec. 1992, *Journal of Applied Mechanics, Transactions of the ASME*, **59**(4), pp. 722-729.

17. Yanyutin, E. G. and Voropai, A. V., "Identification of the Impulsive Load on an Elastic Rectangular Plate," Oct. 2003, *International Applied Mechanics*, **39**(10), pp. 1199-1204.

18. Seydel, R. and Chang, F-K., "Impact Identification of Stiffened Composite Panels: I. System Development," April 2001, *Smart Materials and Structures*, **10**(2), pp. 354-369.

19. Seydel, R. and Chang, F-K., "Impact Identification of Stiffened Composite Panels: II. Implementation Studies," April 2001, *Smart Materials and Structures*, **10**(2), pp. 370-379.

20. Seydel, R. and Chang, F-K., "Real-Time Impact Identification of Stiffened Composite Panels," March 1999, *Proceedings of SPIE – The International Society for Optical Engineering Conference on Smart Structures and Integrated Systems*, 3668(1), pp. 295-305.

21. Tracy, M. and Chang, F-K., "Identifying Impact Load in Composite Plates Based on Distributed Piezoelectric Sensor Measurements," 1996, *Proceedings of SPIE – The International Society for Optical Engineering*, **2717**, pp. 231-236.

22. Choi, K. and Chang, F-K., "Identification of Impact Force and Location using Distributed Sensors," Jan. 1996, *American Institute of Aeronautics and Astronautics Journal*, **34**(1), pp. 136-142.

23. Shih, C. Y., Zhang, Q., and Tatsuno, T., "Force Identification by Using Principle and Modal Coordinate Transformation Method," 1989, *Vibration Analysis – Techniques and Applications, ASME Publication DE 18-4*, pp. 303-309.

24. Zhang, Q., Allemang, R. J., and Brown, D. L., "Modal Filter: Concept and Applications," 1990, *Proceedings of the International Modal Analysis Conference*, **1**, pp. 487-496.

25. Tikhonov, A. N., and Arsenin, Y. V., "Effect of Structural Modes on Vibratory Force Determination by the Pseudo Inverse Technique," 1986, *American Institute of Aeronautics and Astronautics Journal*, **24**, pp. 504-509.

26. Okubo, N., Tanabe, S., and Tatsuno, T., "Identification of Forces Generated by a Machine Under Operating Condition," 1985, *Proceedings of the International Modal Analysis Conference*, **2**, pp. 920-927.

27. Karlsson, S. E. S., "Identification of External Structural Loads from Measured Harmonic Responses," 1996, *Journal of Sound and Vibration*, **196**(1), pp. 59-74.

28. Rider, E. and Day, M. J., "The Indirect Measurement of Force Excitations in Vibrating Systems – an Experiment," July 1988, *Proceedings of the Sixth British Conference on The Teaching of Vibration and Noise, Sheffield Polytechnic*, pp. 163-173.

29. Hillary, B., *Indirect Measurement of Vibration Excitation Forces*, 1983, *Ph.D. dissertation*, Department of Mechanical Engineering, Imperial College, London.

30. Lloyd, S. J., *An Assessment of Modal Analysis Techniques for Force Determination in Open-Coupled Systems*, 1987, *MSc dissertation*, Royal Naval Engineering College, Mandon, Plymouth.

31. Bartlett, F. D. and Flannelly, W. G., "Modal Verification of Force Determination for Measuring Vibratory Loads," April 1979, *Journal of the American Helicopter Society*, **24**, pp. 10-18.

32. Giasante, N., Jones, R. and Calapodas, N. J., "Determination of In-flight Helicopter Loads," July 1983, *Journal of the American Helicopter Society*, **27**, pp. 58-64.

33. Kinns, R., McColl, J. H., and McKinstry, J., "Use of Forced Response Measurements for the Estimation of Machine Source Properties," 1983, *Proceedings of Internoise, Edinburgh*, pp. 475-478.

34. Tikhonov, A. N., Goncharsky, A. V., Stepanov, V. V., and Yagola, A. G., "Regularizing Algorithms and a Priori Information," 1983, Moscow: Nauka, (in Russian).

35. Filippov, A. P. and Sklyar, V. A., "Transverse Impact Against a Rectangular Plate in View of Rotary Inertia and Shearing Forces," 1972, forces," *Dinam. Prochn. Mashin, Izd. Khar'kov. Univ.*, Kharkov, **14**, pp. 12-19.

36. Greenwood, D. T., *Principles of Dynamics*, 2nd ed. Upper Saddle River, New Jersey: PTR Prentice Hall, 1988.

37. Adams, D. E. and Brown, D. L., "Estimation of Rigid Body Frequency Response Function Matrices via Redundant Perimeter Reference Measurements", 1995, *Proceedings of the International Modal Analysis Conference*, pp. 1231-1241.